

Original Article

Enhanced delivery of anti-inflammatory therapeutics using pH-responsive histidine-modified poly-L-lysine on mesoporous silica nanoparticles

Zuliar Permana¹, Jovinka N. Xeliem¹, Normalita F. Zefrina¹, Latifa F. Hanum¹, Ni LPKV. Nirmalayanti¹, Benny Permana² and Diky Mudhakar^{1*}

¹Department of Pharmaceutics, School of Pharmacy, Institut Teknologi Bandung, Bandung, Indonesia; ²Department of Pharmacochemistry, School of Pharmacy, Institut Teknologi Bandung, Bandung, Indonesia

*Corresponding author: mudhakar@itb.ac.id

Abstract

Mesoporous silica nanoparticles (MSNs) are effective platforms for drug delivery due to their high surface area, adjustable pore sizes, and biocompatibility. The aim of this study was to explore the application of histidine-modified poly-L-lysine (PLL-His) as a pH-responsive gatekeeper to control the release of an anti-inflammatory agent, celecoxib, from MSNs. MSNs were synthesized through a sol-gel process using cetyltrimethylammonium bromide (CTAB) as a template and were functionalized with amine groups using (3-aminopropyl)triethoxysilane (APTES). Drug loading was achieved via adsorption in ethanol. Subsequently, poly-L-lysine (PLL) and PLL-His were conjugated to the MSNs using 1-ethyl-3-(3-dimethylaminopropyl)carbodiimide (EDAC) and N-hydroxysuccinimide (NHS) to form MSN-NH₂-Drug-PLL and MSN-NH₂-Drug-PLL-His constructs. Characterization of these particles was conducted using Fourier-transform infrared (FT-IR) spectroscopy, Brunauer-Emmett-Teller (BET) analysis, and particle size analysis. Results showed that the particle size of MSN-NH₂-drug-PLL and MSN-NH₂-drug-PLL-His was 237.10±6.56 nm and 234.03±14.65 nm, respectively, indicating suitability for cellular uptake. BET analysis confirmed the increased surface area and pore volume after the removal of CTAB, demonstrating successful mesopore formation. Drug release tests were performed in simulated gastric (pH 1.2) and physiological (pH 7.4) conditions, showing that PLL-His-modified MSNs exhibited minimal release in acidic conditions and sustained release at physiological pH. The PLL-His effectively functioned as a pH-responsive gatekeeper, enhancing drug targeting and reducing premature release. This study highlights the potential of PLL-His-modified MSNs as a promising model for pH-sensitive, targeted drug delivery, with potential applications across various therapeutic areas requiring precise release profiles. This approach could significantly improve therapeutic outcomes and patient compliance, particularly in disease contexts where pH variability is a critical factor. Overall, the integration of PLL-His as a pH-responsive gatekeeper represents a significant advancement in the design of smart drug delivery systems.

Keywords: Mesoporous silica nanoparticles, pH-responsive drug delivery, histidine-modified poly-L-lysine, controlled release system, targeted drug delivery

Introduction

Inflammation is a complex biological process initiated by the body's immune system in response to various stimuli, such as pathogens, damaged cells, or toxic compounds. While the acute



inflammatory response is crucial for defending the body and initiating tissue repair, its manifestations, such as increased body temperature, redness, swelling, and pain, can become harmful when inflammation persists and becomes chronic [1]. Chronic inflammation is implicated in numerous diseases, such as arthritis, cardiovascular diseases, and cancer, underscoring the need for effective management strategies to mitigate its detrimental effects.

Non-steroidal anti-inflammatory drugs (NSAIDs) are widely used to manage inflammation and pain. Among them, celecoxib (CXB), a selective cyclooxygenase-2 (COX-2) inhibitor, is particularly effective in reducing pain and inflammation in conditions such as osteoarthritis, rheumatoid arthritis, ankylosing spondylitis, and acute pain episodes [2]. Unlike non-selective NSAIDs, which inhibit both COX-1 and COX-2 and often lead to gastrointestinal side effects, CXB specifically targets COX-2, making it a safer option for long-term use [2]. However, prolonged use of CXB still poses challenges, such as the need for frequent dosing to maintain therapeutic levels and potential gastrointestinal irritation [2]. Therefore, advanced drug delivery system that can provide controlled and sustained release of CXB is a considerable interest to improve patient compliance and minimize side effects. Slow-release drug formulations have been developed to maintain a consistent drug concentration in the bloodstream or target tissues by controlling the release rate [3]. Among the emerging approaches, the encapsulation of drugs in nanoparticle systems has shown significant promise. Mesoporous silica nanoparticles (MSNs) have gained attention due to their unique properties, including high surface area, tunable pore sizes, excellent biodegradability, and biocompatibility, which make them suitable candidates for drug delivery applications [4]. MSNs work by providing a porous structure that can encapsulate therapeutic agents, protecting them from degradation and allowing for controlled release [4]. By modifying the surface of MSNs with specific molecules or polymers, it is possible to control the drug release rate, either slowing it down or enhancing it [4]. This surface modification can be tailored to respond to various stimuli such as pH, temperature, or enzymes, thereby achieving targeted and sustained drug delivery [4].

To further improve control over drug release, MSNs can be functionalized with "gatekeepers" that prevent premature drug release and protect the drug from interactions with non-target environments. Gatekeepers can be designed to respond to various stimuli, such as pH changes, enzymes, light, or temperature, ensuring targeted and responsive drug delivery. For oral drug delivery, it is essential that the drug remains protected from the acidic stomach environment (pH 1.2–3.5) and is released in the intestine (pH 5.5–7.4) [5,6]. This selective drug release can be achieved using pH-responsive gatekeepers. Poly-L-lysine (PLL) is a cationic polymer that has been extensively studied as a functionalizing agent for MSNs in various drug delivery applications, including gene delivery [7]. PLL-functionalized MSNs have demonstrated good biocompatibility and biodegradability [7]. Researchers have explored modifications of PLL to enhance its properties as a gatekeeper, particularly by incorporating histidine residues [8]. Histidine-modified PLL has been shown to improve pH-responsiveness, reduce cytotoxicity, and enhance drug release characteristics compared to unmodified PLL [8,9]. The presence of the protonated imidazole group in histidine provides enhanced pH sensitivity, making it a more effective gatekeeper for controlled drug release [9]. Despite the promising potential of histidine-modified PLL in gene delivery, its application in drug delivery systems involving MSNs, particularly for the controlled release of NSAIDs like CXB, remains underexplored. The aim of this study was to develop and characterize a novel drug delivery system using MSNs loaded with CXB, employing histidine-modified PLL as a pH-responsive gatekeeper. The goal is to achieve controlled and targeted drug release, thereby enhancing therapeutic efficacy of CXB and improving patient compliance in the treatment of chronic inflammation.

The development of a pH-responsive drug delivery system using histidine-modified PLL as a gatekeeper for MSNs loaded with CXB represents a significant advancement in nanomedicine. By addressing the challenges of frequent dosing and gastrointestinal side effects associated with conventional NSAID therapy, this innovative approach has the potential to enhance the management of chronic inflammatory conditions. Moreover, this strategy could serve as a versatile model for other therapeutic applications requiring targeted release profiles, paving the way for broader use of nanoparticle-based drug delivery systems in precision medicine.

Methods

Synthesis of mesoporous silica nanoparticles (MSNs)

MSNs were synthesized using a modified sol-gel method. A reaction mixture was prepared by combining 70 mL of distilled water and 20 mL of ethanol in a 100 mL. To this mixture, 0.2 g of cetyltrimethylammonium bromide (CTAB) (Sigma-Aldrich, St. Louis, MO, USA) was added as a structure-directing agent, followed by the addition of 0.27 mL of ammonia, which acted as a catalyst. The mixture was stirred in a water bath at 40°C and 200 rpm for 30 minutes (mins) to ensure homogeneity and micelle formation. After the initial stirring, 1 mL of tetraethyl orthosilicate (TEOS) (Sigma-Aldrich, St. Louis, MO, USA) was added dropwise as a silica precursor to initiate condensation and nanoparticle formation. The reaction was allowed to proceed under controlled conditions of 40°C and 200 rpm for 24 hours. The resulting suspension was centrifuged at 5000 rpm for 15 mins to separate the MSN precipitate. The precipitate was washed thoroughly with ethanol to remove residual reactants and dried in an oven at 60°C for 12–24 hours. To remove the CTAB template and expose the mesoporous structure, the dried MSNs were treated with 1 mL of 37% hydrochloric acid in 100 mL of methanol. This mixture was stirred at 60°C for 6 hours to ensure complete template removal. The suspension was centrifuged at 5000 rpm for 15 mins, and the precipitate was collected. The MSNs were washed with ethanol to remove any remaining impurities and dried again at 60°C for 12–24 hours. The final MSN product was weighed to determine yield and stored in a desiccated vial for subsequent functionalization and characterization. The synthesis of MSNs is illustrated in **Figure 1**.

Functionalization of MSNs with amine groups (MSN-NH₂)

Amine functionalization of MSNs was achieved through surface modification using (3-aminopropyl)triethoxysilane (APTES) (Sigma-Aldrich, St. Louis, MO, USA). Briefly, 100 mg of dried MSNs was placed into a 30 mL reaction vial. To this, 19 mL of ethanol and 1 mL of APTES were added. The mixture was stirred at room temperature (25°C) at 200 rpm for 24 hours to allow efficient covalent attachment of amine groups onto the MSN surface. The resulting suspension was centrifuged at 5000 rpm for 15 mins to separate the functionalized nanoparticles. The precipitate was collected, washed thoroughly with ethanol to remove unreacted APTES and by-products, and dried in an oven at 60°C for 6–12 hours. The final weight of the amine-functionalized MSNs (MSN-NH₂) was recorded to determine the efficiency of the functionalization process. The samples were stored in a desiccated vial to preserve their integrity for subsequent use in further modifications and applications. The functionalization of MSN-NH₂ is illustrated in **Figure 1**.

Loading of celecoxib (CXB) into amine-functionalized MSNs (MSN-NH₂-CXB)

Drug loading was performed by dissolving 100 mg of CXB (Novell Pharmaceutical Laboratories, Bogor, Indonesia) and 5 mL of ethanol, achieving a concentration of 20 mg/mL. The solution was sonicated for 30 mins to ensure complete dissolution. Subsequently, 100 mg of MSN-NH₂ was added to the vial containing the CXB solution. The mixture was sonicated for an additional 30 mins to facilitate drug infiltration into the nanopores, followed by stirring with a magnetic stirrer at 400 rpm for 24 hours at room temperature (25°C) to maximize drug loading. After the loading process, the suspension was centrifuged at 5000 rpm for 30 mins to separate the drug-loaded nanoparticles. The resulting precipitate was washed with distilled water to remove any unbound drug, dried in an oven at 40°C, and stored in a sealed vial to obtain CXB-loaded MSN-NH₂ (MSN-NH₂-CXB). This process ensured effective encapsulation of CXB for subsequent evaluation of drug release behavior and therapeutic potential. The drug loading procedure is illustrated schematically in **Figure 1**.

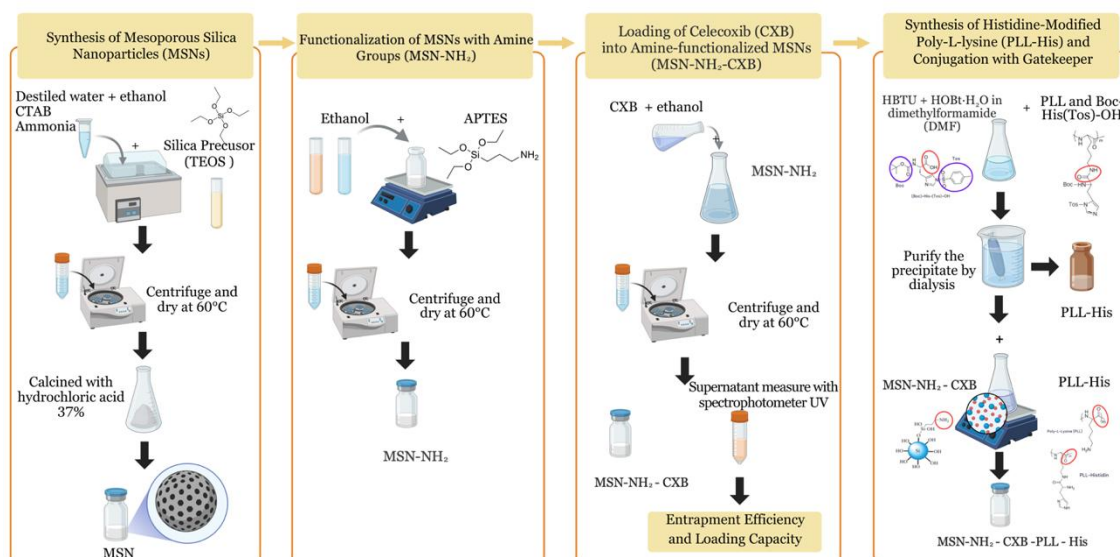


Figure 1. Schematic representation of preparation MSN-NH₂ modified gatekeepers loading CXB.

Determination of entrapment efficiency and loading capacity

The entrapment efficiency and loading capacity of CXB in MSN-NH₂ were evaluated by quantifying the untrapped drug in the supernatant. The loading supernatant was diluted 2000-fold, and the absorbance was measured at 253 nm using a T92+ UV-Visible spectrophotometer (PG Instruments, Lutterworth, UK) [10]. The drug concentration was calculated using a pre-established calibration curve.

Entrapment efficiency (%) was calculated by subtracting the amount of untrapped CXB from the initial amount of CXB, dividing by the initial amount of CXB, and multiplying by 100. Loading capacity (%) was calculated by subtracting the amount of untrapped CXB from the initial amount of CXB, dividing by the amount of MSN used, and multiplying by 100.

Synthesis of histidine-modified poly-L-lysine (PLL-His)

PLL-His was synthesized via a coupling reaction between PLL and Boc-His(Tos)-OH. Briefly, 427 mg of PLL, 803 mg of Boc-His(Tos)-OH, 743 mg of HBTU (O-(benzotriazol-1-yl)-N,N,N',N'-tetramethyluronium hexafluorophosphate), and 300 mg of HOBt·H₂O (1-hydroxybenzotriazole hydrate) were accurately weighed (all from Sigma-Aldrich, St. Louis, MO, USA). HBTU and HOBt·H₂O were dissolved in 10 mL of dimethylformamide (Sigma-Aldrich, St. Louis, MO, USA), and the resulting solution was added to a reaction flask containing PLL and Boc-His(Tos)-OH. The reaction mixture was stirred continuously at room temperature for 15 hours using a magnetic stirrer. After the reaction, the mixture was concentrated under reduced pressure using a rotary evaporator. The crude product was precipitated using a solvent system of diethyl ether and ethyl acetate. To remove impurities, the precipitate was purified by dialysis in a 0.05% trifluoroacetic acid (TFA) solution for 24 hours. The purified product was then freeze-dried to obtain the final PLL-His. The synthesis of PLL-His is depicted in **Figure 1**.

Conjugation of modified MSN-NH₂ with gatekeeper histidine-modified poly-L-lysine (MSN-NH₂-CXB-PLL-His)

The conjugation of PLL-His as a gatekeeper to drug-loaded mesoporous silica nanoparticles (MSN-NH₂-CXB) was achieved using a carbodiimide coupling reaction. For this, 100 mg of PLL-His was activated by reacting with 100 mg of carbodiimide (EDAC) (Sigma-Aldrich, St. Louis, MO, USA) and 60 mg of NHS in 5 mL of distilled water. The mixture was stirred at 400 rpm for 1 hour to activate the carboxylic groups of PLL-His, enabling subsequent covalent bonding. In parallel, 100 mg of MSN-NH₂-CXB was dispersed in 55 mL of dimethylformamide and sonicated for 30 mins to achieve a homogeneous suspension. The activated PLL-His solution was then added dropwise to the MSN-NH₂-CXB suspension under continuous stirring at 400 rpm. The reaction was carried out for 24 hours at room temperature to ensure efficient conjugation. After the reaction, the resulting mixture was centrifuged at 5000 rpm for 15 mins to collect the

conjugated nanoparticles. The sediment was washed thoroughly with distilled water to remove unreacted reagents and by-products. The final product, MSN-NH₂-CXB-PLL-His, was dried at 40°C for 12–24 hours and stored in a sealed vial for further characterization and application. The conjugation steps of MSN-NH₂-CXB-PLL-His are illustrated in **Figure 1**.

Characterization of nanoparticles

The synthesized nanoparticles were systematically characterized to evaluate their physicochemical and structural properties. Particle size, polydispersity index (PDI), and zeta potential were determined using dynamic light scattering (DLS) and zeta potential analysis. These measurements were conducted with a particle size analyzer (Beckman Coulter, West Sacramento, CA, USA) and a zeta potential analyzer (Malvern Instruments, Malvern, UK), ensuring precise and reproducible results. Thermal stability and compositional analysis of mesoporous silica nanoparticles (MSN), amino-functionalized MSN (MSN-NH₂), drug-loaded MSN (MSN-NH₂-CXB), and gatekeeper-modified MSNs were performed using thermogravimetric analysis (TGA) on an STA 7300 simultaneous thermal analyzer (Hitachi High-Tech Science Corporation, Tokyo, Japan). Structural characterization of the gatekeeper-modified MSNs and the gatekeeping materials, poly-L-lysine (PLL) and PLL-His, was conducted using hydrogen nuclear magnetic resonance (¹H-NMR) spectroscopy and Fourier-transform infrared (FT-IR) spectroscopy. ¹H-NMR analysis was carried out using a Bruker NMR spectrometer (Bruker Corporation, Billerica, MA, USA), while FT-IR spectra were obtained with a Jasco FT/IR-4200 type A spectrometer (Jasco Corporation, Tokyo, Japan). These analyses confirmed the successful functionalization and integration of the gatekeeping molecules, providing critical insights into their structural integrity and suitability for pH-responsive drug delivery applications.

In vitro release test

The in vitro release profiles of MSN-NH₂ conjugated with gatekeepers PLL and PLL-His, each loaded with 6.5 mg of CXB, were evaluated under simulated gastric and physiological conditions. Samples were placed into vials containing 25 mL of hydrochloric acid-NaCl buffer (pH 1.2) or phosphate buffer (pH 7.4), both supplemented with 1% sodium lauryl sulfate (SLS) (all from Sigma-Aldrich, St. Louis, MO, USA) to maintain sink conditions. The mixtures were stirred at 100 rpm in a water bath shaker maintained at 37°C to mimic in vivo conditions. At predetermined time intervals, 1 mL aliquots were withdrawn from each vial and immediately replaced with an equal volume of fresh buffer to maintain constant sink conditions. Sink conditions ensured that the concentration of the drug in the solution remained significantly lower than its saturation solubility, which allowed for a consistent and accurate measurement of drug release without saturation effects. For the pH 1.2 medium, samples were collected at 3, 6, 9, 12, 15, 30, 60, and 120 mins, whereas for the pH 7.4 medium, sampling was conducted at 1, 3, 6, 9, and 24 hours. The collected samples were filtered through a 0.45 µm membrane filter (Millipore Sigma, hydrophilic PVDF, Burlington, MA, USA) to remove particulate matter. The concentration of CXB in the filtrate was determined spectrophotometrically using a T92+ UV-Visible spectrophotometer (PG Instruments, Lutterworth, UK) at a wavelength of 253 nm.

Results

Particle size, zeta potential, and polydispersity index (PDI)

The particle size, zeta potential, and PDI of MSNs and their modifications were analyzed to evaluate their potential suitability for drug delivery applications and the results are summarized in **Table 1**. The particle size analysis showed that unmodified MSNs had an initial diameter of 199.50±17.46 nm, which increased to 238.50±7.50 nm upon CXB loading (MSN-CXB), indicating successful drug incorporation into the mesoporous structure. Following amine functionalization, MSN-NH₂ exhibited a reduced size of 182.10±13.62 nm, attributed to structural reorganization after CTAB template removal and amine group introduction. Subsequent CXB loading into amine-functionalized MSNs (MSN-NH₂-CXB) resulted in an increased size of 230.40±8.95 nm. Further surface modifications with PLL and PLL-His yielded particles of 237.10±6.56 nm and

234.03±14.65 nm, respectively. Notably, all formulations maintained sizes below 250 nm, which is optimal for cellular internalization [11].

Surface charge characteristics, measured as zeta potential, demonstrated significant modifications throughout the functionalization process (**Table 1**). The initial negative charge of unmodified MSNs (-18.68±2.48 mV) shifted to positive (+18.94±0.34 mV) after amine functionalization. PLL and PLL-His conjugation further increased the positive charge to +40.89±0.69 mV and +38.15±0.84 mV, respectively, confirming successful surface modification and enhanced colloidal stability (**Table 1**). The increased positive charge can be attributed to the abundant amine groups present in PLL. The polydispersity index remained below 0.5 for all formulations, indicating uniform size distribution and good colloidal stability [12]. Drug loading studies revealed the superior performance of amine-functionalized MSNs compared to their unmodified counterparts. While MSN-CXB showed modest drug entrapment efficiency (6.91±0.29%) and loading capacity (6.89±0.31%), MSN-NH₂-CXB demonstrated significantly higher values for both parameters (entrapment efficiency: 23.35±0.39%; loading capacity: 23.54±0.42%). This enhancement can be attributed to the increased surface interactions between CXB and the amine groups on the modified MSN surface.

Table 1. Characterization of particle size, zeta potential, and polydispersity index (PDI) for mesoporous silica nanoparticles (MSN) and its modifications

Nanoparticles	Particle size (nm)	Zeta potential (mV)	Polydispersity index (PDI)	Entrapment efficiency (%)	Loading capacity (%)
MSN	199.50±17.46	-18.68±2.48	0.19±0.04	NA	NA
MSN-NH ₂	182.10±13.62	+18.94±0.34	0.29±0.05	NA	NA
MSN-CXB	238.5±7.50	-28.79±5.38	0.34±0.05	6.91±0.29	6.89±0.31
MSN-NH ₂ -CXB	230.40±8.95	+21.55±1.78	0.25±0.06	23.35±0.39	23.54±0.42
MSN-NH ₂ -CXB-PLL	237.10±6.56	+40.89±0.69	0.29±0.01	NA	NA
MSN-NH ₂ -CXB-PLL-His	234.03±14.65	+38.15±0.84	0.31±0.02	NA	NA

NA: not available, the sample does not contain CXB, or the characterization of entrapment efficiency and loading capacity was not performed due to the conjugation of PLL/PLL-His with MSN-NH₂ that has already undergone CXB loading.

Fourier-transform infrared (FT-IR) spectroscopy

FT-IR spectroscopy was utilized to confirm the synthesis, functionalization, and conjugation of MSNs and their derivatives. The characteristic Si-O-Si stretching vibrations at 1080 cm⁻¹ confirmed the structural integrity of the silica framework across all formulations (**Figure 2**). The peaks at 802 cm⁻¹ and 964 cm⁻¹, corresponding to Si-O and Si-OH bonds, respectively (**Figure 2A**), validate the formation of silanol groups on the MSN surface. The broad absorption band observed at 3436 cm⁻¹ was attributed to -OH stretching vibrations from surface silanol groups and adsorbed water molecules. The successful removal of the CTAB surfactant was confirmed by the disappearance of the methylene (-CH₂) stretching vibration peaks at 2927 cm⁻¹ and 2857 cm⁻¹ in the FT-IR spectrum of MSN following extraction with methanol and hydrochloric acid [13]. This critical step ensures the formation of mesopores, enabling the nanoparticles to undergo further functionalization and drug loading.

Following amine functionalization (MSN-NH₂) (**Figure 2B**), new peaks appeared at 2927 cm⁻¹, corresponding to C-H stretching vibrations, and at 1562 cm⁻¹, attributed to NH₂ bending vibrations. The reduction in the intensity of the peak at 964 cm⁻¹ indicated a chemical reaction between surface silanol groups (Si-OH) and the amine precursor, APTES [14]. This reduction is due to the consumption of Si-OH groups as they react with APTES to form Si-O-Si bonds, incorporating the amine groups into the structure [14]. Furthermore, the appearance of additional peaks at 1492 cm⁻¹, corresponding to C-N bonds in amide groups, provides further confirmation of the successful introduction of amine groups onto the MSN surface [15].

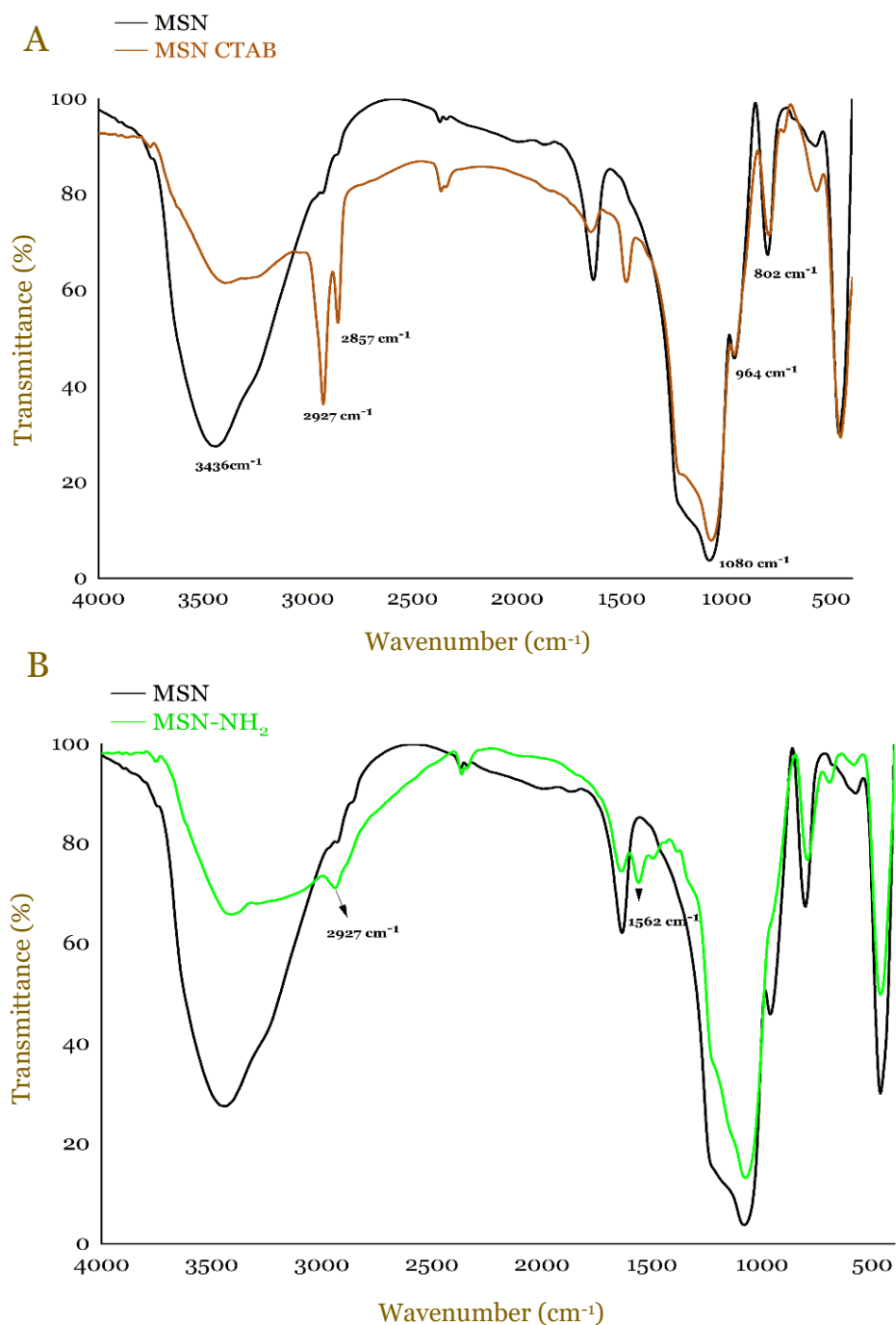


Figure 2. Fourier-transform infrared (FT-IR) spectroscopy spectra showing mesoporous silica nanoparticles (MSN) before and after cetyltrimethylammonium bromide (CTAB) extraction (A) and MSN functionalized with amine groups (MSN-NH₂) (B).

The incorporation of CXB into MSN-NH₂ (MSN-NH₂-CXB) was further confirmed using FT-IR (**Figure 3**). The disappearance of characteristic CXB peaks at 3340 cm⁻¹ and 3234 cm⁻¹, corresponding to N-H stretching vibrations of the NH₂SO₂ group, indicated that the drug was successfully encapsulated within the MSN pores. Furthermore, no new peaks were observed in the MSN-NH₂-CXB spectrum compared to MSN-NH₂, suggesting that the drug was physically adsorbed rather than chemically bonded to the carrier [16,17].

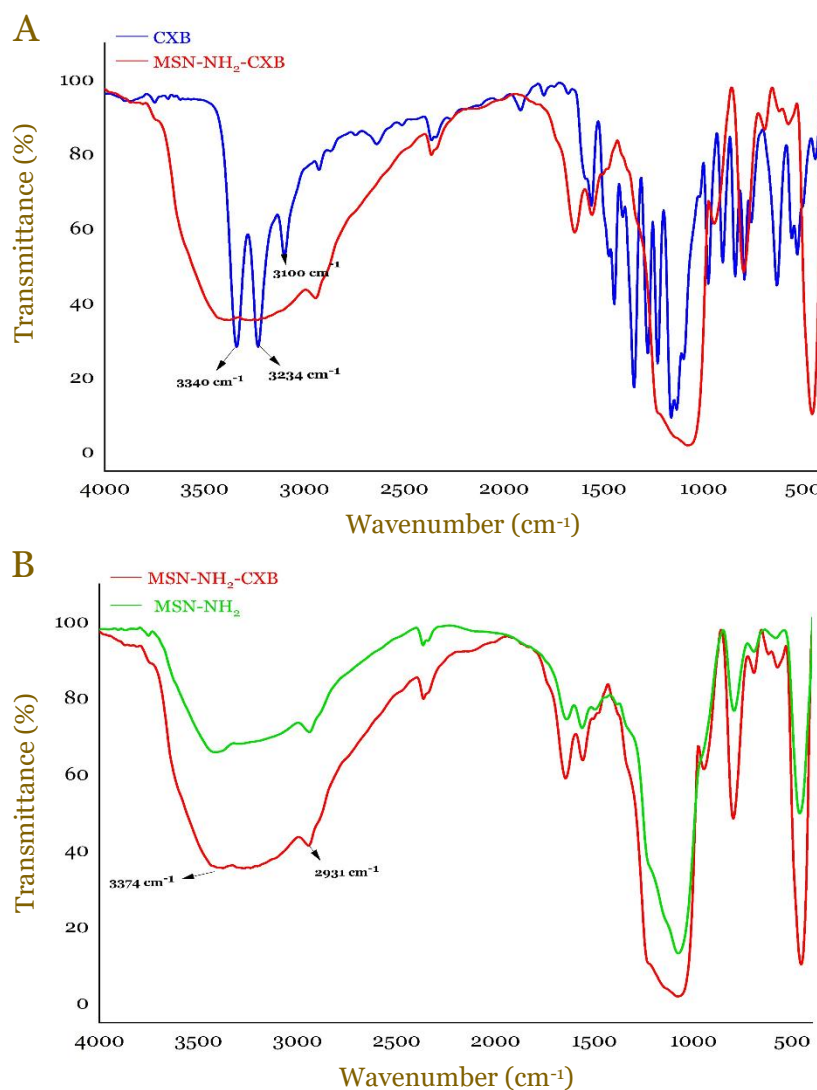


Figure 3. Fourier-transform infrared (FT-IR) spectroscopy spectra confirming the incorporation of celecoxib (CXB) into amine-functionalized MSNs (MSN-NH₂). (A) Comparison of CXB and MSN-NH₂-CXB spectra. (B) Comparison of MSN-NH₂ and MSN-NH₂-CXB spectra.

The conjugation of MSN-NH₂-CXB with gatekeepers PLL and PLL-His was validated by the appearance of Amide I (C=O stretching) and Amide II (N-H bending) peaks at 1650 cm⁻¹ and 1550 cm⁻¹, respectively (**Figure 4A**), in the FT-IR spectra of MSN-NH₂-CXB-PLL and MSN-NH₂-CXB-PLL-His, these peaks are indicative of the formation of amide bonds between the nanoparticles and the gatekeepers. Additionally, the increased intensity of the 1658 cm⁻¹ peak in the PLL-His spectrum corresponds to the aromatic C=N bond in the histidine imidazole ring [18]. This increased intensity is significant as it confirms the successful incorporation of histidine into the PLL structure, enhancing the pH-responsive behavior of the gatekeeper. Peaks at 2923 cm⁻¹ and 2858 cm⁻¹ (**Figure 4B**), characteristic of alkyl groups in PLL and PLL-His, further confirmed the successful conjugation process. The presence of these peaks indicates that the alkyl chains of the polymers are now part of the nanoparticle structure, ensuring that the gatekeepers are firmly attached to the MSNs, which is crucial for controlled drug release.

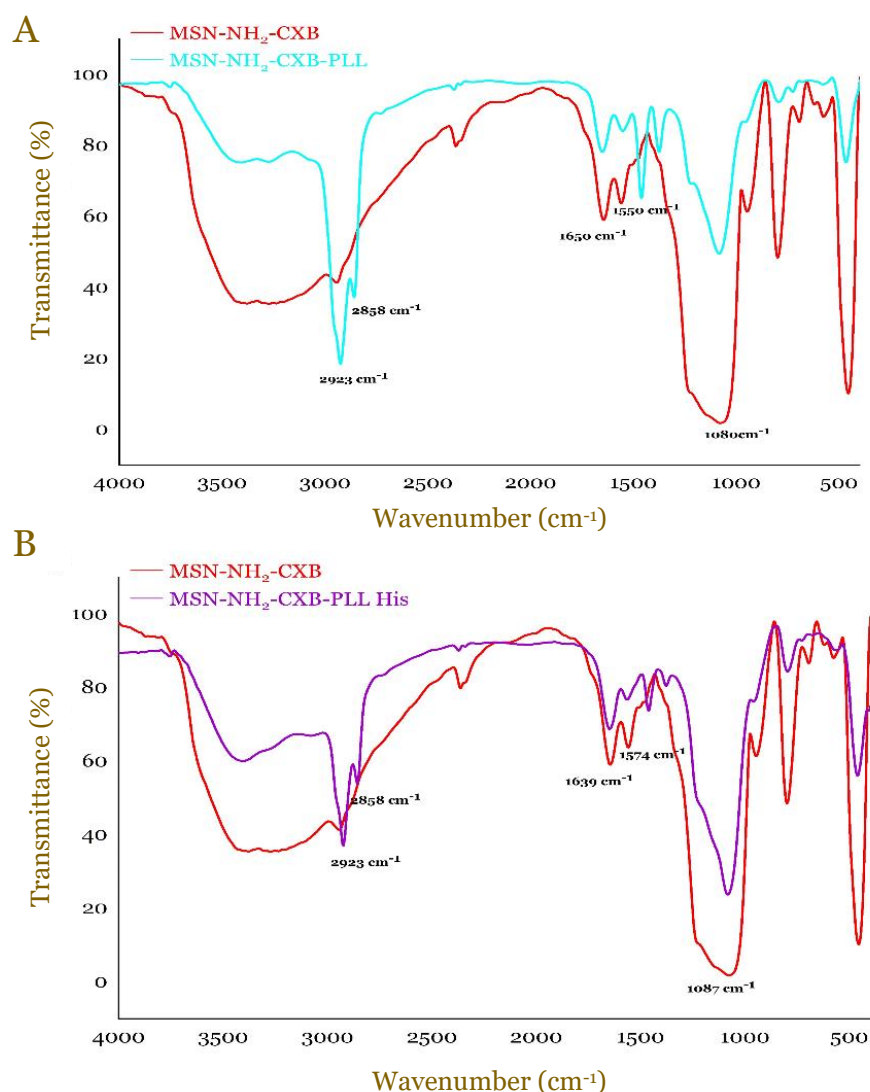


Figure 4. Fourier-transform infrared (FT-IR) spectroscopy spectra of mesoporous silica nanoparticles functionalized with amine groups and loaded with celecoxib (MSN-NH₂-CXB) before and after conjugation with gatekeepers: (A) poly-L-lysine (PLL) and (B) poly-L-lysine-histidine (PLL-His).

Nuclear magnetic resonance (NMR) spectroscopy

The formation of PLL-His was further validated using ¹H-NMR spectroscopy (Figure 5), which complemented the findings from FT-IR analysis. The spectrum of PLL-His displayed distinct new peaks between 7–8 ppm, corresponding to the aromatic protons of the imidazole ring in histidine. These peaks were absent in the ¹H-NMR spectrum of unmodified PLL, providing strong evidence of the successful incorporation of histidine into the PLL backbone via amide bond formation. The chemical shift in the region of 7–8 ppm aligns with reported values for the histidine imidazole group, further supporting the successful modification [19]. This, in conjunction with FT-IR data, highlights the effective functionalization of PLL with histidine, preserving the structural integrity of the poly-L-lysine framework while introducing the desired imidazole functionality. The combined spectroscopic data strongly confirmed the suitability of PLL-His as a gatekeeper for nanoparticle functionalization.

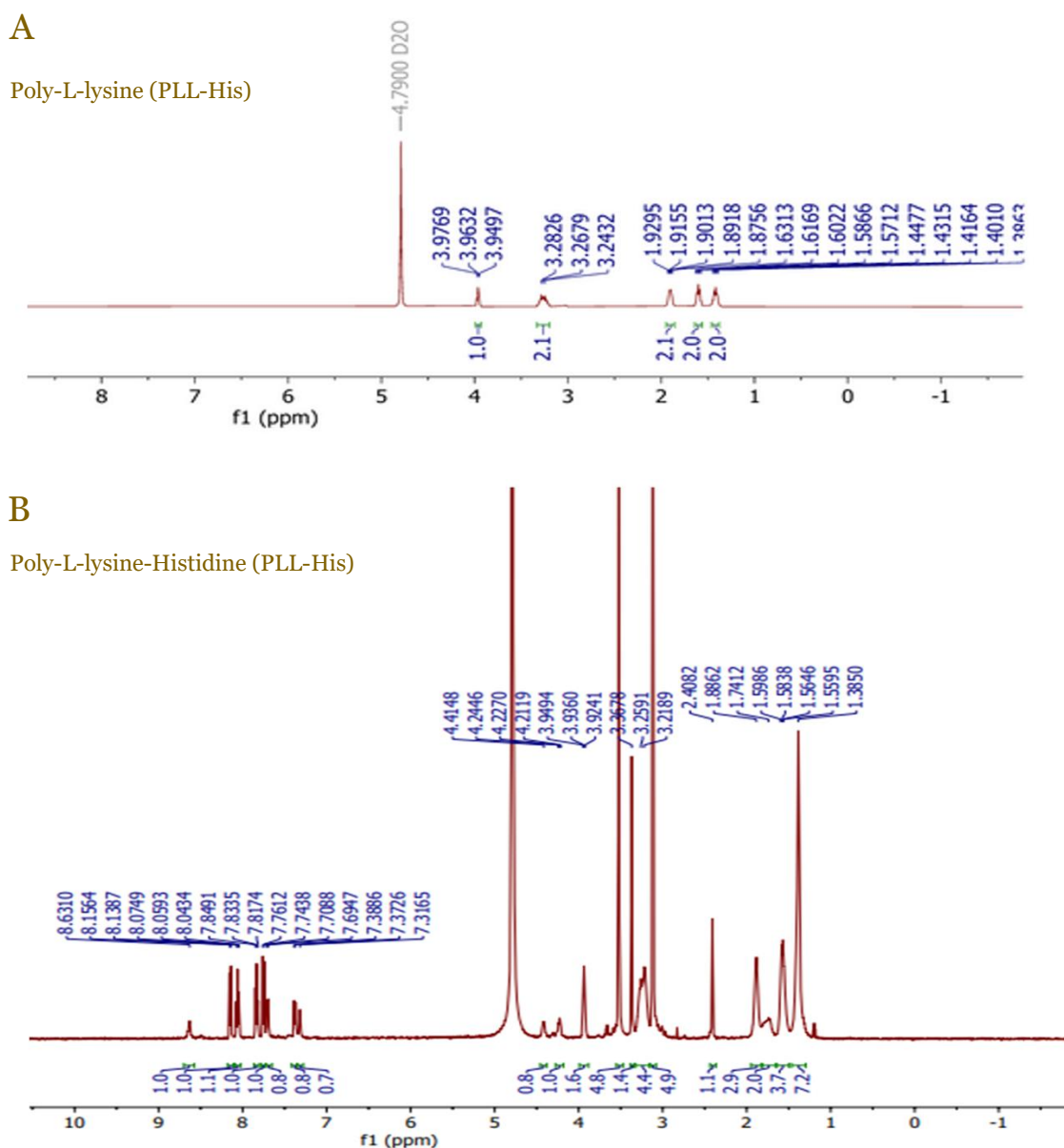


Figure 5. Hydrogen nuclear magnetic resonance ($^1\text{H-NMR}$) spectra of (A) poly-L-lysine (PLL) and (B) histidine-modified poly-L-lysine (PLL-His).

Brunauer-Emmett-Teller (BET) analysis

BET analysis was performed to evaluate the changes in surface area, pore size, and pore volume of MSNs after surfactant removal. The results demonstrated a significant enhancement in the structural properties of MSNs upon successful extraction of the CTAB surfactant (**Table 2**). The surface area increased markedly from 166.77 m^2/g for MSN-CTAB to 897.83 m^2/g after CTAB removal. Similarly, the pore size expanded from 2.42 nm to 4.76 nm, and the pore volume increased from 2.03 cm^3/g to 2.14 cm^3/g (**Table 2**). These findings confirmed the effective removal of the surfactant template and the formation of a well-defined mesoporous structure. The substantial increase in surface area and pore dimensions highlighted the capability of the MSNs to serve as an efficient drug delivery platform, offering high drug-loading capacity and the potential for sustained release applications.

Table 2. Brunauer-Emmett-Teller (BET) analysis of mesoporous silica nanoparticles (MSN) before and after cetyltrimethylammonium bromide (CTAB) removal

Nanoparticles	Surface area (m^2/g)	Pore size (nm)	Pore volume (cm^3/g)
MSN-CTAB	166.77	2.42	2.03
MSN	897.83	4.76	2.14

Thermogravimetric analysis (TGA) of mesoporous silica nanoparticle (MSN) and its modifications

TGA was performed on MSN and their various modifications to assess the successful incorporation of functional groups and drug loading. The thermogravimetric curves, spanning from 0–800°C and normalized at 0°C, provide valuable insights into the compositional changes of the nanoparticles (**Figure 6**). The thermogravimetric curves reveal a progressive increase in mass loss from unmodified MSN to its functionalized counterparts. The initial modification, MSN-NH₂, exhibited a noticeable reduction in mass compared to bare MSN, indicating the successful grafting of amine groups onto the silica surface. This trend continued with the subsequent loading of CXB onto MSN-NH₂, as evidenced by a further decrease in sample mass with increasing temperature. The conjugation of pH-responsive gatekeepers, PLL and PLL-His, to the MSN-NH₂-CXB system, was corroborated by the observed increase in mass loss. Notably, MSN-NH₂-CXB-PLL demonstrated a substantial mass reduction of 49.17%, signifying a significant increase in the organic component within the sample. This observation supported the successful integration of the polymeric gatekeeper onto the nanoparticle surface. The TGA data provided compelling evidence for the stepwise modification of MSN, from amine functionalization to drug loading and gatekeeper attachment. These results confirmed the successful incorporation of organic moieties into the MSN framework, which is crucial for enhancing the functionality and performance of the nanoparticles as drug delivery systems.

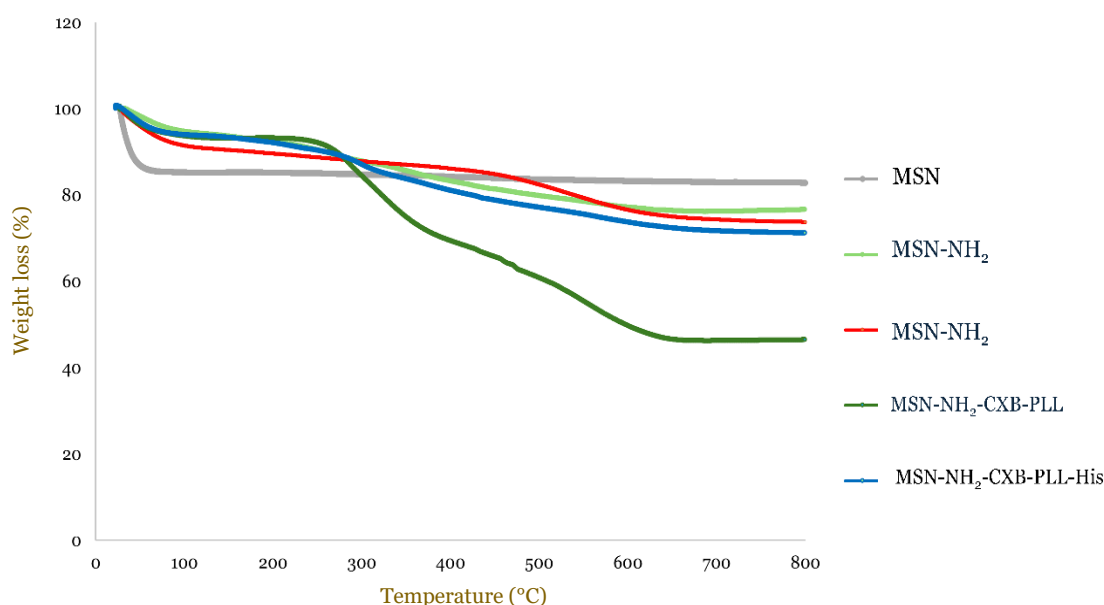


Figure 6. Thermogravimetric analysis (TGA) graph of mesoporous silica nanoparticle (MSN) and its modifications.

In vitro release test

The in vitro release profile of CXB from MSN was evaluated under simulated gastric (pH 1.2) and intestinal (pH 7.4) conditions, revealing a pH-dependent release mechanism influenced by gatekeeper modifications (**Figure 7**). At pH 1.2, the release of CXB from unmodified MSN (MSN-NH₂-CXB) was significantly higher ($16.06 \pm 4.39\%$) compared to MSN modified with PLL or PLL-His (**Figure 7A**). MSN-NH₂-CXB-PLL released only $1.27 \pm 0.013\%$, while MSN-NH₂-CXB-PLL-His released $2.97 \pm 0.498\%$ (unpaired Student t-test, $p < 0.05$). This reduction in drug release for modified systems was attributed to strong electrostatic interactions between the protonated amino groups of PLL or the imidazole groups of PLL-His and the negatively charged MSN surface, which effectively block the MSN pores and minimize CXB release in the acidic gastric environment. Under physiological conditions (pH 7.4), a contrasting release behavior was observed (**Figure 7B**). MSN-NH₂-CXB-PLL-His had a significantly higher cumulative release ($8.24 \pm 0.22\%$) compared to MSN-NH₂-CXB-PLL ($4.06 \pm 0.58\%$) (unpaired Student t-test, $p < 0.05$). This enhanced release can be attributed to the deprotonation of histidine's imidazole

groups at neutral pH, which reduced electrostatic interactions with the MSN surface, allowing PLL-His to release CXB more efficiently. In contrast, PLL remained positively charged at this pH, maintaining stronger interactions with the MSN surface and restricting drug release. This behavior demonstrated that the deprotonation of histidine residues at physiological pH weakened their electrostatic interactions with negatively charged surfaces [8]. Such tunable behavior highlighted the advantage of PLL-His gatekeepers, enabling selective drug release in the intestinal environment. Collectively, these results underscored the dual functionality of gatekeepers in modulating drug release. While PLL and PLL-His effectively prevent CXB release in gastric conditions, their differential response at physiological pH highlighted the superior tunability of PLL-His for targeted drug delivery applications.

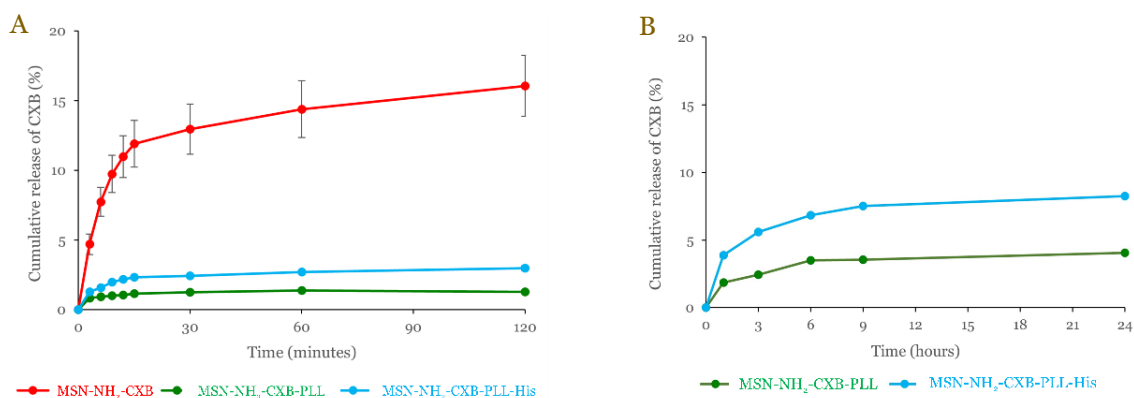


Figure 7. Comparisons of celecoxib (CXB) release profile from mesoporous silica nanoparticles (MSN) comparing release profiles with and without gatekeepers (PLL and PLL-His) at pH 1.2 (A) and pH 7.4 (B).

Discussion

The study focused on improving MSNs for delivering the CXB. We successfully enhanced the drug loading capacity by grafting amine groups onto the surface of the MSNs. Additionally, we effectively modulated the drug release using a specialized gatekeeper, PLL-His. This approach ensured that CXB remains protected in gastric pH conditions and is released in intestinal pH conditions. The successful synthesis and functionalization of MSNs were confirmed through multiple characterization techniques. FT-IR spectroscopy validated the removal of the CTAB surfactant template, a crucial step in exposing the mesoporous structure essential for effective drug loading. BET analysis revealed substantial improvements in structural properties following template removal, with the surface area increasing from 166.77 m²/g to 897.83 m²/g and the pore size expanding from 2.42 nm to 4.76 nm. These findings highlight the successful creation of a mesoporous structure optimized for encapsulating CXB.

Similar structural enhancements have been widely documented in the literature. For instance, lactosaminated MSNs showed improved surface area and pore volume, facilitating superior drug loading and release efficiency [13]. Additionally, studies on aminopropyl-functionalized MSNs and thiol-functionalized MSNs have also demonstrated significant increases in surface area and pore volume, resulting in enhanced drug delivery performance [20,21]. These findings collectively highlighted the effectiveness of various functionalization strategies in optimizing the structural properties of MSNs for improved therapeutic outcomes [13]. The functionalization of MSNs with amine groups further enhanced their drug-loading capacity. MSN-NH₂ exhibited an entrapment efficiency of 23.35±0.39% and a corresponding loading capacity of 23.54±0.42%, significantly outperforming unmodified MSNs. These improvements can be attributed to the strong electrostatic and hydrogen-bonding interactions facilitated by the amine groups, which increase the binding affinity of hydrophobic drugs like CXB to the MSN surface. Prior research supported these findings, demonstrating that amine-functionalized MSNs exhibit higher loading capacities for drugs such as curcumin, further emphasizing the utility of amine functionalization in optimizing MSN-based drug delivery systems [22,23].

The study's *in vitro* drug release profiles underscored the importance of gatekeeper molecules, specifically PLL and PLL-His, in modulating release behavior under varying pH conditions. Minimal drug release was observed at gastric pH (1.2) for PLL-His-modified MSNs ($2.97 \pm 0.498\%$), effectively protecting CXB from degradation in acidic environments. Conversely, at intestinal pH (7.4), PLL-His-modified MSNs demonstrated a significantly higher cumulative drug release ($8.24 \pm 0.22\%$) compared to PLL-coated MSNs ($4.06 \pm 0.58\%$). These observations highlight the effectiveness of histidine residues in PLL-His systems, where deprotonation at neutral pH reduces electrostatic interactions between the gatekeeper and drug molecules, facilitating controlled release from the mesopores. This pH-responsive release behavior aligns with previous findings on histidine-functionalized carriers, which demonstrated superior tunability and responsiveness in drug-delivery systems [24]. In comparison to conventional systems employing non-histidine-based gatekeepers, PLL-His provides superior tunability and responsiveness, addressing limitations in selective drug delivery [25].

PLL is well-known for enhancing cellular uptake through its strong electrostatic interactions with negatively charged cellular membranes. For example, PLL-functionalized MSNs showed a 45% increase in cellular uptake in human lung cancer cells, attributable to favorable charge interactions between the positively charged PLL and the negatively charged cell membranes [26]. Similarly, PLL-functionalized carbon quantum dots exhibited enhanced cellular uptake across multiple cell lines, reinforcing the importance of PLL in improving nanoparticle internalization through electrostatic mechanisms [27]. The integration of histidine residues into PLL-His systems represents a significant advancement in nanoparticle functionalization by addressing the critical challenge of endosomal escape. Histidine's imidazole group, with a pKa (at which the molecule is 50% protonated and 50% deprotonated) of approximately 6.0, becomes protonated under mildly acidic endosomal conditions, triggering the proton sponge effect [8,9,28]. This effect facilitates osmotic swelling, leading to endosomal membrane disruption and the efficient release of encapsulated drugs into the cytoplasm [29-31]. Studies have demonstrated that grafting histidine onto PLL enhances its buffering capacity and improves endosomal escape. For instance, histidine-rich peptides, such as H6 (HHHHHH), have been extensively utilized for their endosomal escape properties, further validating the potential of histidine modifications in intracellular drug delivery [32,33]. Additionally, PLL-His systems mitigate the cytotoxicity associated with highly charged polymers like PLL by reducing excessive positive charge density [34,35]. Histidine residues help to balance the overall charge, minimizing nonspecific interactions with cellular components and improving biocompatibility [35,36]. These dual features of enhanced cellular uptake and efficient endosomal escape make PLL-His-functionalized MSNs a versatile and effective platform for targeted drug delivery applications [8]. The observed precision in drug release and intracellular delivery with PLL-His systems offer distinct advantages over conventional systems lacking histidine modifications. The tunable pH sensitivity and improved biocompatibility of PLL-His-functionalized MSNs make them particularly suitable for addressing challenges in diseases characterized by pH variability, such as cancer and inflammatory conditions. Furthermore, these systems provide enhanced therapeutic efficacy while minimizing off-target effects, making them safer and more effective for clinical translation. Future studies should focus on evaluating the *in vivo* pharmacokinetics, biodistribution, and long-term safety of PLL-His-functionalized MSNs. Integrating additional functional moieties, such as targeting ligands or stimuli-responsive elements, could further broaden the utility of these systems in precision medicine. By combining tunability, biocompatibility, and functionality, PLL-His-modified MSNs represent a transformative advancement in nanopharmaceutical design, offering a versatile and efficient tool for improving therapeutic delivery and clinical outcomes.

Despite the promising results, this study has several limitations. Validation through *in vivo* experiments is needed to confirm the efficacy and safety of PLL-His-functionalized MSNs. Long-term toxicity assessments are crucial to ensure biocompatibility. Additionally, exploring a broader range of pH conditions and therapeutic agents and testing the scalability and reproducibility of synthesis methods are essential for clinical translation. Future research should also investigate other gatekeeping mechanisms to further enhance targeted drug delivery. Addressing these aspects will optimize PLL-His-functionalized MSNs for clinical applications,

potentially advancing treatments for diseases with pH variability, such as cancer and inflammatory conditions.

Conclusion

This study successfully demonstrated the development of a pH-responsive drug delivery system utilizing histidine-modified PLL-His as a gatekeeper for MSNs loaded with CXB. The synthesis and functionalization processes were optimized, resulting in MSNs with significantly enhanced surface area, pore volume, and particle morphology suited for efficient drug encapsulation. Amine functionalization further improved drug loading efficiency, ensuring robust encapsulation of hydrophobic drugs like CXB. The pH-responsive behavior of PLL-His as a gatekeeper allowed precise control over drug release, with minimal premature release in acidic environments and sustained release under physiological conditions. This dual-release mechanism highlighted the efficacy of PLL-His-modified MSNs in protecting the therapeutic agent during gastric transit while ensuring targeted delivery at the desired site. Importantly, the tunable nature of this system offers a valuable foundation for addressing pH-dependent therapeutic challenges. The potential for further functionalization, including the integration of disease-specific targeting ligands or other stimuli-responsive mechanisms, enhances the adaptability of this model for broader therapeutic applications. By addressing limitations such as premature drug release and the need for frequent dosing, this system demonstrates promise for improving patient outcomes through enhanced therapeutic efficacy and reduced systemic side effects. Future research should evaluate the *in vivo* pharmacokinetics and biodistribution of PLL-His-modified MSNs and explore their adaptability to biologics, peptides, and gene therapies to expand their therapeutic potential.

Ethics approval

Not required.

Acknowledgments

The authors wish to thank Ebrahim Saad Ebrahim Sadaqa for his constructive discussion and helpful advice in writing the English manuscript.

Competing interests

All the authors declare that there are no conflicts of interest.

Funding

This study was funded by Institut Teknologi Bandung (ITB) Excellent Research Grant, number 959/IT1.B07.1/TA.00/2024.

Underlying data

Derived data supporting the findings of this study are available from the corresponding author on request.

Declaration of artificial intelligence use

We hereby confirm that no artificial intelligence (AI) tools or methodologies were utilized at any stage of this study, including during data collection, analysis, visualization, or manuscript preparation. All work presented in this study was conducted manually by the authors without the assistance of AI-based tools or systems.

How to cite

Permana Z, Xeliem JN, Zefrina NF, *et al.* Enhanced delivery of anti-inflammatory therapeutics using pH-responsive histidine-modified poly-L-lysine on mesoporous silica nanoparticles. *Narra J* 2025; 5 (1): e1815 - <http://doi.org/10.52225/narra.v5i1.1815>.

References

1. Chen L, Deng H, Cui H, *et al.* Inflammatory responses and inflammation-associated diseases in organs. *Oncotarget* 2017;9(6):7204-7218.
2. Gong L, Thorn CF, Bertagnolli MM, *et al.* Celecoxib pathways: Pharmacokinetics and pharmacodynamics. *Pharmacogenet Genomics* 2012;22(4):310-318.
3. Alasvand N, Urbanska AM, Rahmati M, *et al.* Therapeutic nanoparticles for targeted delivery of anticancer drugs. In: Grumezescu AM, editor. *Multifunctional systems for combined delivery, biosensing and diagnostics*. Amsterdam: Elsevier Inc.; 2017.
4. Jadhav, Ps D, Vv P. Mesoporous silica nanoparticles (MSN): A nanonetwork and hierarchical structure in drug delivery. *J Nanomed Res* 2015;2(5):156-161.
5. Cui M, Zhang M, Liu K. Colon-targeted drug delivery of polysaccharide-based nanocarriers for synergistic treatment of inflammatory bowel disease: A review. *Carbohydr Polym* 2021;272(6):118530.
6. Hadji H, Bouchemal K. Advances in the treatment of inflammatory bowel disease: Focus on polysaccharide nanoparticulate drug delivery systems. *Adv Drug Deliv Rev* 2022;114101;1-20.
7. Santhamoorthy M, Ramkumar V, Thirupathi K, *et al.* L-lysine functionalized mesoporous silica hybrid nanoparticles for pH-responsive delivery of curcumin. *Pharmaceutics* 2023;15(6):1-17.
8. Zhao GX, Tanaka H, Kim CW, *et al.* Histidinylated poly-L-lysine-based vectors for cancer-specific gene expression via enhancing the endosomal escape. *J Biomater Sci Polym Ed* 2014;25(5):519-534.
9. Midoux P, Pichon C, Yaouanc JJ, *et al.* Chemical vectors for gene delivery: A current review on polymers, peptides and lipids containing histidine or imidazole as nucleic acids carriers. *Br J Pharmacol* 2009;157(2):166-178.
10. Mudhakar D, Sadaqa E, Permana Z, *et al.* Dual-functionalized mesoporous silica nanoparticles for celecoxib delivery: Amine grafting and imidazolyl PEI gatekeepers for enhanced loading and controlled release with reduced toxicity. *Molecules* 2024;29:3456:1-18.
11. Foroozandeh P, Aziz AA. Insight into cellular uptake and intracellular trafficking of nanoparticles. *Nanoscale Res Lett* 2018;13:339.
12. Sadaqa E, Utami RA, Mudhakar D. In vitro cytotoxic and genotoxic effects of *Phyllanthus niruri* extract loaded chitosan nanoparticles in TM4 cells and their influence on spermatogenesis. *Pharmacia* 2024;71:1-14.
13. Quan G, Pan X, Wang Z, *et al.* Lactosaminated mesoporous silica nanoparticles for asialoglycoprotein receptor targeted anticancer drug delivery. *J Nanobiotech* 2015;13(7):1-12.
14. Zaharudin NS, Isa EDM, Ahmad H, *et al.* Functionalized mesoporous silica nanoparticles templated by pyridinium ionic liquid for hydrophilic and hydrophobic drug release application. *J Saudi Chem Soc* 2020;24(3):289-302.
15. Lee NK, Park SS, Ha CS. pH-sensitive drug delivery system based on mesoporous silica modified with poly-L-lysine (PLL) as a gatekeeper. *J Nanosci Nanotechnol* 2020;20(11):6925-6934.
16. Alajami HN, Fouad EA, Ashour AE, *et al.* Celecoxib-loaded solid lipid nanoparticles for colon delivery: Formulation optimization and in vitro assessment of anti-cancer activity. *Pharmaceutics* 2022;14(1):131.
17. Günaydin Ş, Yılmaz A. Improvement of solubility of celecoxib by inclusion in MCM-41 mesoporous silica: Drug loading and release. *Turkish J Chem* 2015;39(2):317-333.
18. Paramanatham P, Antony AP, Lal SBS, *et al.* Antimicrobial photodynamic inactivation of fungal biofilm using amino functionalized mesoporous silica-rose bengal nanoconjugate against *Candida albicans*. *Sci African* 2018;1:e00007.
19. Ajikumar A, Premkumar AKN, Narayanan SP. The self-assembly of L-histidine might be the cause of histidinemia. *Sci Rep* 2023;13(1):1-9.
20. Yang P, Gai S, Lin J. Functionalized mesoporous silica materials for controlled drug delivery. *Chem Soc Rev* 2012;41(9):3679-3698.
21. Wang Y, Zhao Q, Han N, *et al.* Mesoporous silica nanoparticles in drug delivery and biomedical applications. *Nanomedicine* 2015;11(2):313-327.
22. Iranshahy M, Hanafi-Bojd MY, Aghili SH, *et al.* Curcumin-loaded mesoporous silica nanoparticles for drug delivery: Synthesis, biological assays and therapeutic potential - a review. *RSC Adv* 2023;13(32):22250-22267.
23. Estevão BM, Miletto I, Hioka N, *et al.* Mesoporous silica nanoparticles functionalized with amino groups for biomedical applications. *Chem Open* 2021;10(12):1251-1259.
24. Johnson RP, John JV, Kim I. Poly(L-histidine)-containing polymer bioconjugate hybrid materials as stimuli-responsive theranostic systems. *J Appl Polym Sci* 2014;131(18):9029-9040.
25. Bilalis P, Tziveleka LA, Varlas S, *et al.* pH-sensitive nanogates based on poly(L-histidine) for controlled drug release from mesoporous silica nanoparticles. *Polym Chem* 2016;7(7):1475-1485.

26. Wang X, Zhang H, Jing H, *et al.* Highly efficient labeling of human lung cancer cells using cationic poly-L-lysine-assisted magnetic iron oxide nanoparticles. *Nanomicro Lett* 2015;7(4):374-384.
27. Vibhute A, Nille O, Kolekar G, *et al.* Fluorescent carbon quantum dots functionalized by poly L-lysine: Efficient material for antibacterial, bioimaging and antiangiogenesis applications. *J Fluoresc* 2022;32(5):1789-1800.
28. Nelson DL, Cox MM. *Lehninger principles of biochemistry*, Sixth Edition. New York: WH. Freeman; 2012.
29. Sadaqa E, Satrialdi, Kurniawan F, Mudhakar D. Mechanistic insights into endosomal escape by sodium oleate-modified liposomes. *Beilstein J Nanotechnol* 2024;15:1667-1685.
30. Varkouhi AK, Scholte M, Storm G, *et al.* Endosomal escape pathways for delivery of biologicals. *J Cont Rel* 2011;151(3):220-228.
31. Chonn A, Cullis PR. Recent advances in liposome technologies and their applications for systemic gene delivery. *Adv Drug Deliv Rev* 1998;30(1-3):73-83.
32. Hwang HS, Hu J, Na K, *et al.* Role of polymeric endosomolytic agents in gene transfection: A comparative study of poly (L-lysine) grafted with monomeric L-histidine analogue and poly(L-histidine), *Biomacromol* 2014;15:3577-3586.
33. López-Laguna H, Cubarsi R, Unzueta U, *et al.* Endosomal escape of protein nanoparticles engineered through humanized histidine-rich peptides. *Sci China Mater* 2020;63(4):644-653.
34. Luo D, Saltzman WM. Enhancement of transfection by physical concentration of DNA at the cell surface. *Nat Biotechnol* 2000;18(8):893-895.
35. Lv H, Zhang S, Wang B, Cui S, *et al.* Toxicity of cationic lipids and cationic polymers in gene delivery. *J Cont Rel* 2006;114(1):100-109.
36. Akinc A, Thomas M, Klibanov AM, *et al.* Exploring polyethylenimine-mediated DNA transfection and the proton sponge hypothesis. *J Gene Med* 2005;7(5):657-663.